

PAPER • OPEN ACCESS

Modeling of paths and energy losses of high-energy ions in single-layered and multilayered materials

To cite this article: D I Tishkevich *et al* 2020 *IOP Conf. Ser.: Mater. Sci. Eng.* **848** 012089

View the [article online](#) for updates and enhancements.

You may also like

- [Microstructural Effects on the Corrosion Behavior of High-Strength Al–Zn–Mg–Cu Alloys in an Overaged Condition](#)
Joachim Wloka and Sannakaisa Virtanen
- [Strain-stress relationship and dislocation evolution of W–Cu bilayers from a constructed \$n\$ -body W–Cu potential](#)
W Wei, L Chen, H R Gong *et al.*
- [Effect of Cu Content and Aging Conditions on Pitting Corrosion Damage of 7xxx Series Aluminum Alloys](#)
Shan-Shan Wang, I-Wen Huang, Li Yang *et al.*

ECS
The
Electrochemical
Society
Advancing solid state &
electrochemical science & technology

DISCOVER
how sustainability
intersects with
electrochemistry & solid
state science research

Modeling of paths and energy losses of high-energy ions in single-layered and multilayered materials

D I Tishkevich^{1,2}, S S Grabchikov¹, E A Grabchikova¹, D S Vasin¹, S B Lastovskiy¹, A S Yakushevich¹, D A Vinnik², T I Zubar^{1,2}, I V Kalagin³, S V Mitrofanov³, D V Yakimchuk⁴ and A V Trukhanov^{1,2}

¹Laboratory of Magnetic Films Physics, Scientific-Practical Materials Research Centre of National Academy of Sciences of Belarus, P. Brovki str. 19, Minsk, 220072, Belarus

²Laboratory of Single Crystal Growth, South Ural State University, Lenin ave. 76, Chelyabinsk, 454080, Russia

³Nuclear Reactions Laboratory, Joint Institute of Nuclear Research, J. Curi str. 6, Dubna, 141980, Russia

⁴Cryogenic Research Department, Scientific-Practical Materials Research Centre of National Academy of Sciences of Belarus, P. Brovki str. 19, Minsk, 220072, Belarus
E-mail: dashachushkova@gmail.com

Abstract. Modern electronic systems and equipment used in aerospace and nuclear technology, as well as many scientific and medical devices, are used under the influence of a wide range of ionizing radiation (electrons, protons, heavy charged particles etc.). Protons or heavy charged particles exposure can lead to failures in the operation of spacecrafts electronic devices, which is associated with the radiation effects occurrence in an integrated circuits. One of the most effective ways to solve this problem is protection by radiation shields. Linear and mass paths of protons and Ar⁺ ions in Al, Al₂O₃, Bi, and W_{77,7}Cu_{22,3} composite shields were calculated using a SRIM software package. It is shown that the protection efficiency against high-energy ions by materials with large atomic charge values (*Z*) is higher from the position of linear ranges of particles, and lower from the position of mass ranges than materials with low *Z* values. The dependence of the threshold energy on the serial number of particles for Al, Bi and W_{77,7}Cu_{22,3} composite shields is determined. The effect of the sequence in the arrangement and layer thicknesses in the Bi/Al/Al₂O₃ multilayered structures on the protection efficiency against high-energy ions was studied.

1. Introduction

During developing of new materials used in the elements and equipment of aerospace application, it is necessary to provide requirements for resistance to the effects of various types of ionizing radiation (IR). The influence of protons or heavy high-energy ions can lead to sudden failures in the operation of electronic devices and spacecraft (SC) units, which is associated with the occurrence of radiation effects in integrated circuits (ICs) (a single failure and burnout, snapping, etc.) [1]. The solution of this problem is a very complex and multi-level task. In practice, to increase the radiation reliability of electronic components, as a rule, are used: constructive-technological (circuitry) design methods, "majorization" (the creation of a second, third, etc. in an IC – back-up, which in case of failure of the



first one will replace it) and constructive protection (constructive elements of the SC, specialized bodies, local protection) [1, 2].

Often, to provide radiation protection of the spacecraft's electronic components from the effects of electrons and protons of the Earth's radiation belts (ERB), plates or coatings in the form of local protection are used that are formed on individual elements of electronic equipment [3-7]. However, there is an opinion [8], according to which protection against exposure of heavy high-energy ions, (the term heavy charged particles (HCP) is often used in the scientific literature) by using radiation shields is ineffective, since flows of secondary particles and fragments of matter, created by the interaction of HCP with shields material, may have a more negative effect than primary radiation. At the same time, it is known [9] that the fluxes of protons and ERB electrons are relatively stable, and the IR spectra are determined for the main near-Earth orbits. The fluxes of solar cosmic rays (SCR) and galactic cosmic rays (GCR) are unstable factors and are probabilistic in nature. SCR fluxes mainly consist of low-energy electrons and protons ($E \sim 1$ keV) with a density of 10^8 – 10^9 $\text{cm}^{-2}\text{s}^{-1}$, however, during solar flares, the energies can reach 10^8 – 10^9 eV [10]. Protons predominate in the composition of GCR fluxes ($E \leq 10^{12}$ eV), the remaining nuclei account for less than 10%. GCR fluxes are characterized by a relatively low density – up to 5 $\text{cm}^{-2}\text{s}^{-1}$, but possess enormous energy up to 10^{20} eV [11]. According to the data of [12], the energy spectrum of particles in outer space can be characterized by the following values of particle fluxes per 1 mm^2 per year: ~ 30 particles with $E = 10$ GeV, $\sim 7 \cdot 10^{-3}$ particles with $E = 1$ TeV, $\sim 1 \cdot 10^{-6}$ particles with $E = 1$ PeV.

In near-Earth space, the GCR energy spectrum differs significantly from the GCR spectrum in interstellar space, which is associated with the influence of the solar wind (heliosphere) and the Earth's magnetic field. Moreover, the influence of these factors on particles with energies above $10Z$ GeV (Z is the charge of atomic nuclei) is insignificant. On the other hand, electronic components are usually located inside the spacecraft behind the outer body and constructive elements. Therefore, in near-Earth orbits, the energy and the number of particles acting on the electronic components will be lower than those given above, and the issue of protecting electronic components from high-energy ions through the use of radiation shields is of great practical interest. In this regard, the problem of studying the interaction of HCP with protective shields materials is very relevant. Experimental studies require expensive accelerators capable of accelerating ions to enormous energies, therefore, computer simulation of the ions transmission of a given energy in various materials (software packages SRIM, GEANT4, SuperMC etc.) are widely used. This paper presents calculations of the ranges and energy losses of high-energy ions in single-layered and multilayered materials using the SRIM software package.

2. Modeling technique

The linear ranges and energy losses of ions were calculated using SRIM – 2013.00 program [13], in which the model of continuous deceleration is used to simulate the transmission of HCPs in a substance. As high-energy impacts, protons, He^+ , C^+ , Ne^+ , Ar^+ , Fe^+ , Kr^+ and Xe^+ ions with energies from 10 MeV to 27.4 GeV were used. All ions were directed perpendicular to the shields surface. The number of particles in the simulation was 10^3 ions. Linear, mass ranges and threshold energies (E_{thr}) were fixed along the most probable path length of high-energy ions. Single-layered shields based on Al, Al_2O_3 , Bi, $\text{W}_{77.7}\text{Cu}_{22.3}$ composite and Bi/Al/ Al_2O_3 multilayered structures with different sequences and thicknesses of individual layers were as model objects. The shield thickness based on Al, Al_2O_3 and Bi was 1.4 mm, and the thickness of the $\text{W}_{77.7}\text{Cu}_{22.3}$ composite shields was 1.5 mm. The multilayered structures of the four types had the following structure:

- Bi/Al/ Al_2O_3 and Al/ Al_2O_3 /Bi with partial layer thicknesses: Bi – 0.6 mm, Al – 0.2 mm, Al_2O_3 – 0.6 mm and total thickness 1.4 mm;
- Bi/Al/ Al_2O_3 /Bi/Al/ Al_2O_3 /Bi/Al/ Al_2O_3 and Al/ Al_2O_3 /Bi/Al/ Al_2O_3 /Bi/Al/ Al_2O_3 /Bi with partial layer thicknesses: Bi – 0.2 mm, Al – 0.067 mm, Al_2O_3 – 0.2 mm and total thickness 1.4 mm.

3. Results and discussion

Linear range (R) – the distance traveled by a particle in a substance to a complete stop. With an increase in the charge of atomic nuclei in the shield from Al, Bi and $\text{W}_{77.7}\text{Cu}_{22.3}$ composite, linear

ranges decrease. Accordingly, the energies required for the particles to pass through the shields of a given thickness (d) increase with Z rising. The increase in the ions linear ranges with a change in the shield material in the sequence $W_{77.7}Cu_{22.3}$, Bi and Al are primarily due to the lower density of the materials. According to the data of [2], the relative density (ρ) for Al = 2.7, Al_2O_3 = 3.9, Bi = 9.8 and the $W_{77.7}Cu_{22.3}$ composite 17.02 g/cm³. Along with linear ranges, the quantity – mass range (R_M) = $R\rho$, its dimension g·cm⁻² is often used.

The calculated linear and mass ranges of protons and Ar⁺ ions in shields from Al, Al_2O_3 , Bi and $W_{77.7}Cu_{22.3}$ composite are shown in Tables 1 and 2, respectively. It should be noted that the protection effectiveness against HCP by materials with large Z values is higher than materials with low Z , from the position of particle linear ranges (linear shield thickness). From the standpoint of mass ranges (mass shields thickness), materials with low Z have more effective protection than materials with large Z values. From the presented results it also follows that the values of the energies of Ar⁺ ions at which $R \leq d$ for shields from Al, Bi and $W_{77.7}Cu_{22.3}$ composite with thicknesses $d_{Al} = d_{Bi} = 1.4$ mm and $d_{W_{77.7}Cu_{22.3}} = 1.5$ mm are 2.0; 3.16 and 4.77 GeV, respectively.

Table 1. Proton linear and mass ranges in Al, Al_2O_3 , Bi and $W_{77.7}Cu_{22.3}$ composite.

E , MeV		10	15	16	20	23.5	31
Al $Z=13$	R , cm	0.063	0.127	0.136	-	-	-
	R_m , g/cm ²	0.167	0.343	0.367	-	-	-
Al_2O_3 $Z=13;8$	R , cm	0.039	0.080	-	0.133	-	-
	R_m , g/cm ²	0.153	0.313	-	0.518	-	-
Bi $Z = 83$	R , cm	0.035	-	-	0.109	0.135	-
	R_m , g/cm ²	0.345	-	-	1.068	1.323	-
$W_{77.7}Cu_{22.3}$ $Z=74;29$	R , cm	0.019	0.036	-	0.058	-	0.116
	R_m , g/cm ²	0.279	0.541	-	0.870	-	1.752

Table 2. Ar⁺ ions linear and mass ranges in Al, Al_2O_3 , Bi and $W_{77.7}Cu_{22.3}$ composite.

E , GeV		1.0	1.4	2.0	2.6	3.16	4.77
Al $Z=13$	R , cm	0.046	0.077	0.139	-	-	-
	R_m , g/cm ²	0.123	0.207	0.375	-	-	-
Al_2O_3 $Z=13;8$	R , cm	0.028	0.049	0.088	0.139	-	-
	R_m , g/cm ²	0.109	0.189	0.342	0.542	-	-
Bi $Z = 83$	R , cm	0.023	-	0.067	0.098	0.139	-
	R_m , g/cm ²	0.229	-	0.655	-	1.362	-
$W_{77.7}Cu_{22.3}$ $Z=74;29$	R , cm	0.012	-	0.036	-	-	0.148
	R_m , g/cm ²	0.187	-	0.539	-	-	2.235

The results presented in Tables 1, 2 are usually described by the well-known Bethe-Bloch formula [8, 11], according to which the main energy losses of ions with $E > 2$ MeV/nucleon in a substance are associated with ionization losses. Based on the Bethe-Bloch formula, the ionization losses are proportional to the squared charge of the particle's core (Z_i) and proportional to the charge of the atomic nucleus of the material. Consequently, the HCP ranges are reduced in the case of heavier HCP and materials of the medium with Z large values.

The distribution profiles of high-energy C⁺, Ne⁺, Ar⁺, Kr⁺ and Xe⁺ ions in the studied materials have a pronounced peak, the so-called Bragg peak (Figure 1) [14]. The Bragg peak nature is related to the nature of the distribution of absorbed energy along the mean free range in the substance. The main effect of energy absorption occurs at the end of the particle linear mean free range, and the cross section of this process grows with a drop in energy, as a result of which the particle loses the bulk of the energy before it stops. The proton distribution profiles have a completely different form (Figure 1 d, e, f) – the particle flux is scattered in different directions. The proton trajectory is significantly affected by multiple scattering effects. The deviation of the particle from the initial direction is proportional to the number of collisions, depending on the serial number and energy of the HCP.

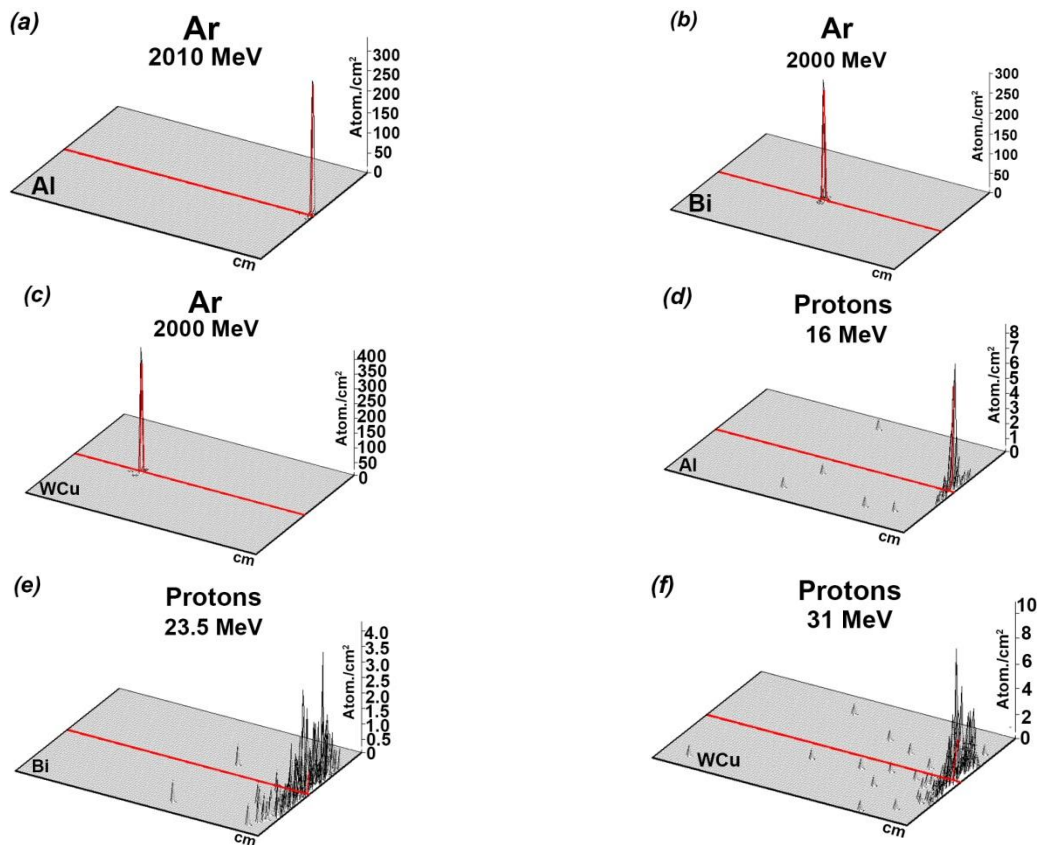
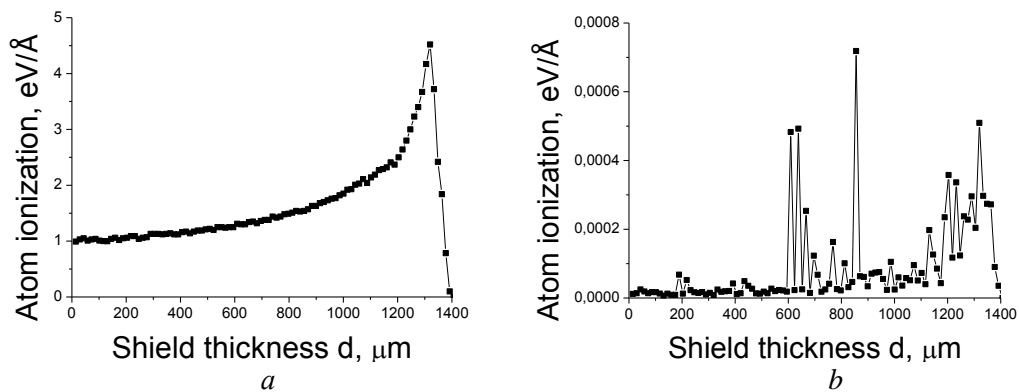


Figure 1. Ar⁺ ions (a, b, c) and protons (d, e, f) histograms of the distribution in shields from Al (a, d), Bi (b, e) and W_{77.7}Cu_{22.3} composite (c, f).

The obtained results are due to the interaction mechanisms of high-energy ions with matter and the associated losses of HCP energy (elastic collisions with substance atoms $E < 10^4$ eV, ionization losses at $E = 10^4$ - 10^8 eV and losses due to nuclear reactions at $E > 100$ MeV/nucleon [11]). Figure 2 shows the ionization losses spectra (a) and nuclear reactions (b) during the transmission of protons with 22.5 MeV energy and Kr⁺ ions with 9.23 GeV energy through 1.4 mm Bi shield. It can be seen that for protons and Ar⁺ ions, the contribution to the energy losses from the ionization process is much higher ($\sim 10^2 - 10^3$) than the contribution from nuclear reactions.



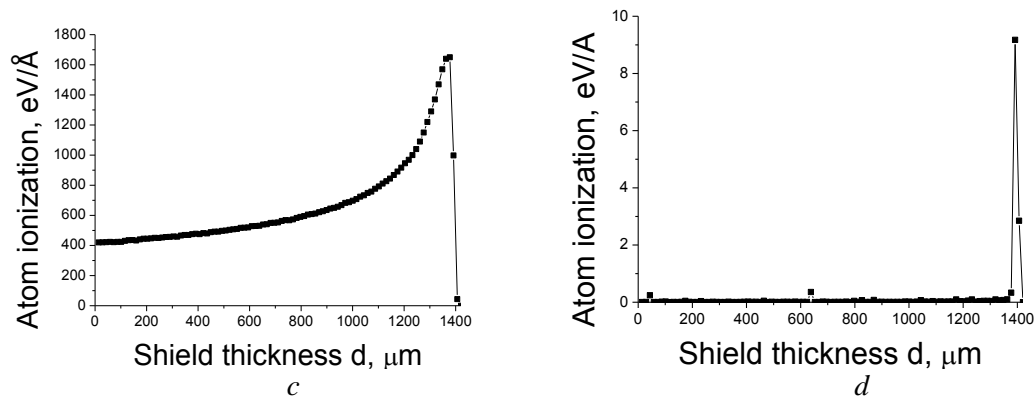


Figure 2. The spectra of ionization losses (a, b) and nuclear reactions (b, d) during the protons transmission with 22.5 MeV (a, b) energy and Kr⁺ ions with 9.23 GeV energy (b, d) through Bi shield with 1.4 mm thickness.

For radiation protection shields, of great interest is the parameter – the threshold ion energy (E_{tsh}), at which the linear range length is equal to the shield thickness. The calculations performed the high-energy protons, He⁺, C⁺, Ne⁺, Ar⁺, Fe⁺, Kr⁺ and Xe⁺ ions ranges in Al, Bi and W_{77.7}Cu_{22.3} composite shields and make it possible to plot the dependence of E_{tsh} on the HCP serial number (Figure 3). As can be seen from the above data, the shields based on the W_{77.7}Cu_{22.3} composite exhibit the highest efficiency from the position of particle linear ranges. The threshold energies for this material with 1.5 mm thickness ($d_m = 2.26 \text{ g/cm}^2$) when exposed to proton and He⁺, C⁺, Ne⁺, Ar⁺, Fe⁺, Kr⁺ and Xe⁺ ions are 37; 480; 790; 1780; 4770; 7900; 14200 and 27000 MeV, respectively. The dependence of the threshold energy on the W_{77.7}Cu_{22.3} composite linear thickness for Ar⁺ ions is shown in Figure 4.

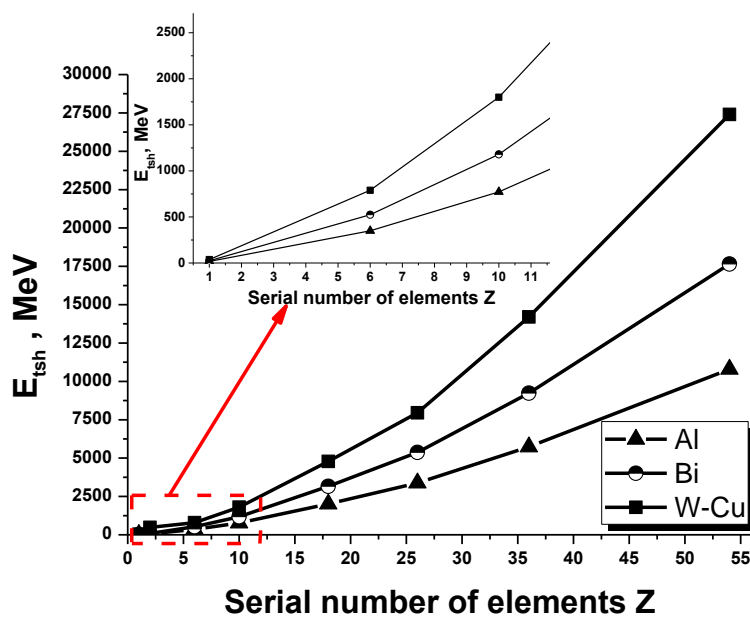


Figure 3. Threshold energy of shields based on Al, Bi and W_{77.7}Cu_{22.3} composite with 1.5 mm thickness for protons, He⁺, C⁺, Ne⁺, Ar⁺, Fe⁺, Kr⁺ and Xe⁺ ions.

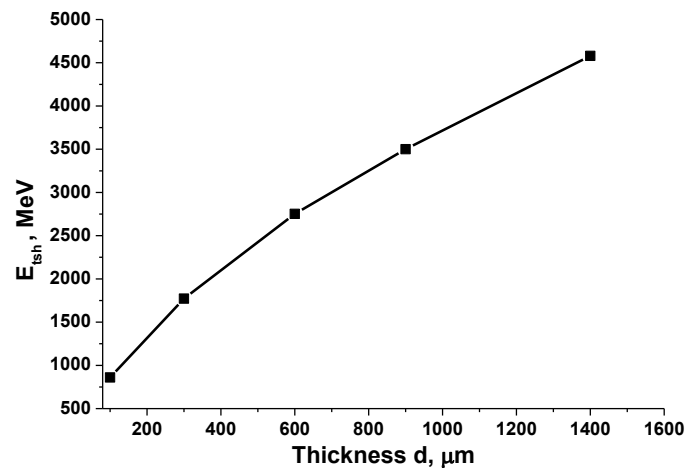


Figure 4. Threshold energy depending on the $W_{77,7}Cu_{22,3}$ composite thickness for Ar^+ ions.

The effect of multilayered structure in shields, namely, the sequence of arrangement and layers thickness, on the protection efficiency against high-energy ions, was studied on the $Bi/Al/Al_2O_3$ structures. Kr^+ ions ($Z = 36$) with an increased contribution of ionization processes to the total energy losses were selected as the acting particles. The calculated dependences of the linear ranges of Kr^+ ions on the number and layers sequence of arrangement of light and heavy elements in $Bi/Al/Al_2O_3$ multilayered structures are presented in Figure 5. For comparison, the same figure shows the simulation results for single-layered Al and Bi shields. From the linear particle ranges position, Al shields are the least effective, Bi shields are the most effective, and multilayered structures are located between them. In the three-layered $Bi/Al/Al_2O_3$ structures, the character of the dependences $R = R(E)$ is determined by the arrangement of individual layers sequence:

- in the case of the $Bi/Al/Al_2O_3$ structure, the $R = R(E)$ dependence up to 0.6 mm ($E \sim 5.4$ GeV) ranges coincides with a similar dependence for pure Bi, since this range corresponds to the thickness of the Bi layer of the multilayered structure. At energies $E > 5.4$ GeV, HCP penetrate into Al_2O_3 and Al layers, whose braking power is lower than that in Bi, as a result of which the efficiency of $Bi/Al/Al_2O_3$ shields at energies $E > 5.4$ GeV is lower than in single-layered Bi. The threshold energy for such structures is 8.1 GeV;

- in the case of the $Al/Al_2O_3/Bi$ structure, the starting point on the graph $R = R(E)$ corresponds to a 0.2 mm ($E = 2$ GeV) linear range and is equal to the thickness of the first Al layer. Therefore, this point coincides with that for single-layered Al. With a further increase in energy due to large losses in the Al_2O_3 layer, the curve $R = R(E)$ of the multilayered structure falls below the curve of single-layered Al. The third Bi layer reinforces this tendency and, with a 1.4 mm final thickness, the linear range approaches the range values for the $Bi/Al/Al_2O_3$ structure. The threshold energy for these structures is 7.9 GeV;

- in the case of the nine-layered $Bi/Al/Al_2O_3/Bi/Al/Al_2O_3/Bi/Al/Al_2O_3$ structure, a large number of layers and their small thicknesses neutralize the effects of different energy absorption by individual layers. It can be concluded that with an increase in layers number, the dependence of linear ranges on the ion energy approaches that shield of equivalent three-layered $Bi/Al/Al_2O_3$ material. Therefore, the dependence $R = R(E)$ for the nine-layered structure is located between the similar curves for the $Bi/Al/Al_2O_3$ and $Al/Al_2O_3/Bi$ structures.

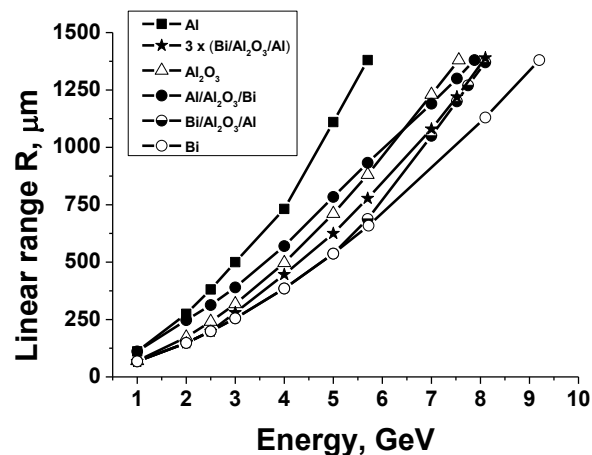


Figure 5. Dependences of linear ranges on the energy of Kr^+ ions in three-layered $\text{Bi}/\text{Al}_2\text{O}_3/\text{Al}$ and $\text{Al}/\text{Al}_2\text{O}_3/\text{Bi}$ structures; nine-layered structure $\text{Bi}/\text{Al}_2\text{O}_3/\text{Al}/\text{Bi}/\text{Al}_2\text{O}_3/\text{Al}/\text{Bi}/\text{Al}_2\text{O}_3/\text{Al}$; single-layered Al and Bi shields.

A value of $R = 0.8$ mm, which corresponds to the thickness of two Al and Al_2O_3 layers requires 5.2 GeV ion energy and a value of $R = 1.4$ mm requires 7.9 GeV an energy for the $\text{Al}/\text{Al}_2\text{O}_3/\text{Bi}$ structures. Therefore, for the transmission through the Bi layer, the ions needed an additional energy of $E = 2.7$ GeV. For the $\text{Bi}/\text{Al}/\text{Al}_2\text{O}_3$ structure a value of $R = 0.6$ mm, which corresponds to the thickness of the Bi layer, requires an ion energy of about 5.4 GeV, and a value of $R = 1.4$ mm – 8.1 GeV. Therefore, for the transmission through Al and Al_2O_3 layers, an additional energy of 2.8 GeV was required. A different level of energy absorption by layers of a three-layered structure depending on their sequence is confirmed by ionization losses spectra calculated when protons with 20 MeV energy (a, b) and Kr^+ ions with 7.75 GeV energy (c, d) pass through multilayered $\text{Bi}/\text{Al}/\text{Al}_2\text{O}_3$ and $\text{Al}_2\text{O}_3/\text{Al}/\text{Bi}$ structures with a 1.4 mm total thickness (Figure 6).

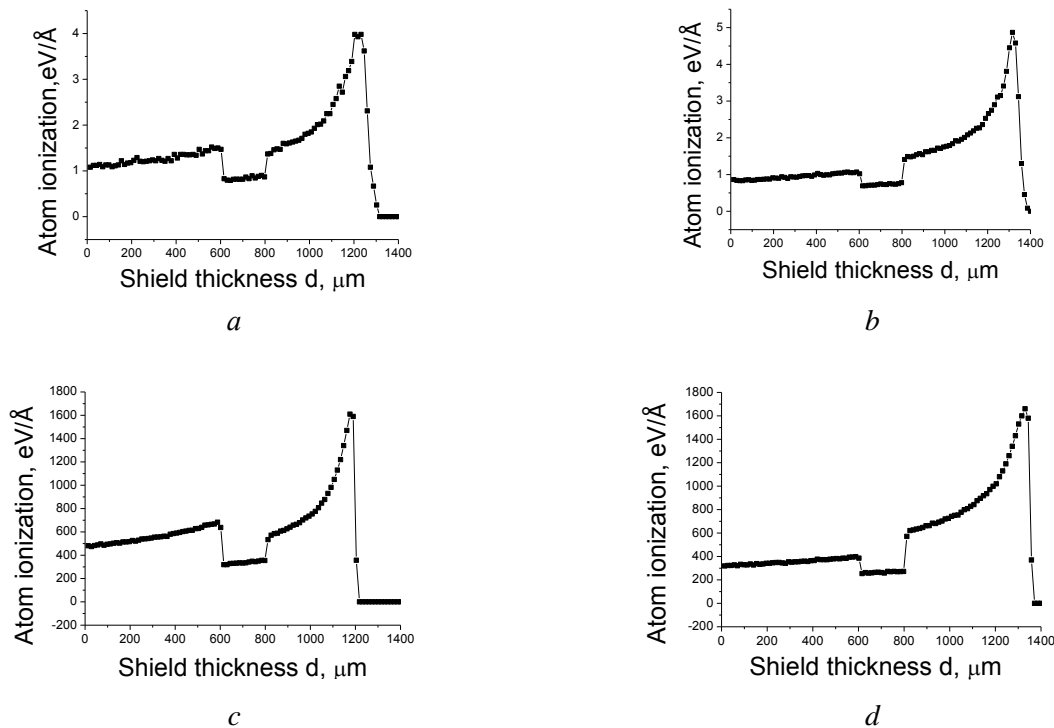


Figure 6. The ionization losses spectra for the protons transmissions with 20 MeV (*a, b*) energy and Kr^+ ions with 7.75 GeV (*c, d*) energy through the $\text{Bi}/\text{Al}/\text{Al}_2\text{O}_3$ (*a, c*) and $\text{Al}_2\text{O}_3/\text{Al}/\text{Bi}$ (*b, d*) multilayered structures with 1.4 mm thickness.

From the data presented in Figure 6, it is clearly seen that the ionization losses for both protons and Kr^+ ions in the case of a multilayered structure, the first layer of which contains a heavy element (Bi), is higher than in the case when the first layer consists light elements (Al, Al_2O_3). It should also be noted that 20 MeV proton energy and the Kr^+ ion energy of 7.75 GeV are practically sufficient for high-energy particles to transmit through the $\text{Al}_2\text{O}_3/\text{Al}/\text{Bi}$ multilayered structure, but not enough to pass through the $\text{Bi}/\text{Al}/\text{Al}_2\text{O}_3$ structure. Thus, in the three-layered $\text{Bi}/\text{Al}/\text{Al}_2\text{O}_3$ structure the character of the $R(E)$ dependences and ionization energy losses are determined by the individual layers arrangement sequence, which can be explained by different levels of ionization losses in layers containing heavy and light elements. Therefore, structures in which the first layer contains a heavy element have more effective protective properties among multilayer shields with respect to monochromatic and high-energy ions. This is a Bi layer for the $\text{Bi}/\text{Al}_2\text{O}_3/\text{Al}$ structure. An increase in the number of layers does not contribute to rise in the shielding efficiency of high-energy ions. Similar results were obtained in [15]. The calculation in the GEANT4 program of 6 MeV proton spectra when transmitting through W/Al two-layered shields with 50 μm individual layer thickness showed that the nature of the conversion of proton spectra depends on the material of first layer. The main transformation of the proton spectrum occurs in the heavy element layer, therefore, the changes in the relative fluxes of proton energy after passing through the W/Al and Al/W shields were 0.275 and 0.318 units, respectively. With an increase in the number of layers to 10, the relative energy flux of the transmitted ions approached 0.305, which corresponded to the W/Al alloy.

4. Conclusion

The linear and mass ranges of protons and Ar^+ ions in Al, Al_2O_3 , Bi and $\text{W}_{77.7}\text{Cu}_{22.3}$ composite shields were calculated. It has been shown that the protection effectiveness against high-energy ions by materials with large values of the Z atomic nuclei charge is higher from the position of particles linear ranges and lowers from the position of mass ranges than materials with low Z values.

The dependence of the threshold energy on the HCP sequence number for shields based on Al, Bi and $W_{77.7}Cu_{22.3}$ composite was determined, according to which shields based on $W_{77.7}Cu_{22.3}$ composite have the highest efficiency from the standpoint of linear particle ranges. The threshold energies for this material with 1.5 mm thickness (2.55 g/cm^2) with exposure of protons and He^+ , C^+ , Ne^+ , Ar^+ , Fe^+ , Kr^+ and Xe^+ are 37; 480; 790; 1780; 4770; 7900; 14200 and 27000 MeV, respectively.

The calculation of the ionization losses spectra for 20 MeV protons and 7.75 GeV Kr^+ ions during passing through multilayered Bi/Al/ Al_2O_3 and Al/ Al_2O_3 /Bi structures showed that the braking of high-energy particles in the case when the first layer contains a heavy element higher than when the first layer contains a light element.

The effect of sequence in the arrangement and layer thickness in multilayered Bi/Al/ Al_2O_3 structure on the protection effectiveness against HCP was studied. It is shown that the nature of the dependences $R(E)$ and ion energy losses are determined by the sequence of individual layers arrangement, which is associated with the difference in the conversion of the spectra by the first layer material. More significant changes in the spectra occur in the layer with the heavy element, since the ionization losses in it are higher, and a higher level of energy flux attenuation corresponds to the case of heavy element/light element shield alternating layers.

Acknowledgement

The work was carried out with financial support of State program of scientific research "Physical Materials Science, New Materials and Technologies" subprogram "Nanomaterials and Nanotechnologies" (task 2.34), Belarusian Republican Foundation for Fundamental Research (BRFFR-JINR Grant No. $\Phi 18\text{Д}-007$), Grant of World Federation of Scientists (Geneva, Switzerland).

References

- [1] Sexton F W 2003 Destructive single-event effects in semiconductor devices and ICs *IEEE Transactions on Nuclear Science* **50** (3) 603.
- [2] J H Heo, B J Ko, B J Chung 2009 A calculation of the cosmic aadiation dose of a semiconductor in a Geostationary orbit satellite depending on the shield thickness *Journal of the Korean Institute of Electrical and Electronic Material Engineers* **22** (6) 476.
- [3] RAD-COAT protection. Available at: <http://www.spaceelectronics.com> (accessed 18 December 2019).
- [4] RAD-PAK protection. Available at: <http://www.maxwell/products/microelectronics> (accessed 18 December 2019).
- [5] WALOPACK protection. Available at: <http://www.3d-plus.com> (accessed 18 December 2019).
- [6] J P Spratt, B C Passenheim, R E Leadon, S Clark, D J Strobel 1997 Effectiveness of IC shielded packages against space radiation *IEEE Transactions on Nuclear Science* **44** (6) 2018.
- [7] T M Jordan, E G Stassinopoulos 1989 Effective radiation reduction in Space Station and missions in the magnetosphere *Advance Space Research* **9** 261.
- [8] M Durante 2011 Physical basis of radiation protection in space travel *Reviews of modern physics* **83** 1245.
- [9] Battison R, Fiandrini E, Sodano P 2002 Study of cosmic rays fluxes in low Earth orbit (LEO) observed with the AMS experiment (Madrid) p. 166.
- [10] J P Spratt, C Conger, R Bredthauer, W Byers, R Groulx, R E Leadon, H Clark 2006 Proton damage effects in high performance P-channel CCDs *IEEE Transactions on Nuclear Science* **53** (2) 423.
- [11] J P Spratt, E A Burke, J C Pickel, R E Leadon 2001 Modeling high-energy heavy-ion damage in silicon *IEEE Transactions on Nuclear Science* **48** (6) 2136.
- [12] J P Spratt, G L Schnable, J D Standeven 1970 Impact of the radiation environment on integrated-circuit technology *IEEE Journal of Solid-State Circuits* **5**(1) 14.
- [13] SRIM-2013. Available at: <http://www.srim.org/SRIM/SRIM-2013> (accessed 18 December 2019).
- [14] M Yamaguchi, Yu Nagao, N Kawachi 2019 A simulation study on estimation of Bragg-peak shifts via machine learning using proton-beam images obtained by measurement of secondary

electron bremsstrahlung *IEEE Transactions on Radiation and Plasma Medical Sciences* DOI: 10.1109/TRPMS.2019.2928016.

- [15] A B Aziz, F Rahman, M H Prodhan Comparison of lead, copper and aluminum as gamma radiation shielding material through experimental measurements and simulation using MCPN version 4c *International Journal of Contemporary Research and Review* **9 (8)** 20193.